PERIODICA POLYTECHNICA SER. CIV. ENG. VOL. 44, NO. 2, PP. 179–196 (2000)

LONG-TERM LOADING EXAMINATIONS IN CONNECTION WITH THE LAW OF LINEAR CREEP

György BALÁZS* and Nguyen Huu THANH**

* Technical University of Budapest, Hungary
Dept. of Building Materials and Engineering Geology
** VIMPEX Ltd., Hungary
Corresponding author: tel: +36-1-463-2226, fax: +36-1-463-3450
E-mail address: balazsvasbeton.vbt.bme.hu

Received: March 30, 2000

Abstract

The failure process of concrete is usually described by the relative volume change function. The initial part of this function is constant. BALÁZS has named the upper limit of the constant part σ_{ka} (lower critical stress). His hypothesis is that, until this point is valid the law of linear creep. With the reviewed pre-experiments we examined the validity of this hypothesis. Due to this reason high strength concrete was long-term loaded up to 30; 50; 62 and 75% of the prism strength and the properties of the concrete were examined.

According to the experiment the law of linear creep is probably valid until $0.50 R/R_{c,pr}$ value, but it has to be proved by further experiments.

Keywords: high strength concrete, long-term loading, creep, law of linear creep.

1. Short Literature Review

FERET [1] has already stated that the compressive strength of concrete is a function of the volume ratio of the constituents and air understood as one of the constituents. The water-cement ratio law of ABRAMS [2], the water-air-cement factor of PALOTÁS [3] meant one newer one step in taking into consideration the structure of concrete more precisely. 30 years ago UJHELYI and BALÁZS realized the significance of the paste saturation at the same time. UJHELYI based his concrete design method on this, while under the leadership of BALÁZS [5], the young scientists of Department of Building Materials at the Technical University of Budapest were doing a research about the connection between the paste saturation and the properties of concrete.

Part of the cement paste covers the surface of the particles with a thin layer while the other part fills the gaps between the particles. In the case the paste is just enough to cover the surface of the particles and to fill the gaps, then the concrete is cement paste saturated. If the cement paste is less, then the concrete is under-saturated, in any other case it is over-saturated.

For designing the concrete to be paste saturated we must know inevitably the gap volume of the aggregate. For concretes with natural sandy gravel aggregate

(MSA=8–63 mm) UJHELYI, for sand concretes (MSA=1–4 mm) THANH [6], [10], [11] and for crushed aggregates ZSIGOVICS [7] introduced formulas to determine the gap volume of the aggregates.

THANH [10] described the paste content, filling the gap volume as the theoretical paste saturation ($V_{p.th}$), and the optimal paste content regarding the strength of concrete as the practical paste saturation ($V_{p,pr}$). During the researches made with mortars, the gap volume of the aggregate structure (theoretical paste saturation) was determined. It was shown that for the Semi Plastic and Plastic sand concrete the water demand of the aggregate can be expressed by the formula of:

$$w_a = 3.4\sqrt{S} + w_0; \text{ (m\%)},$$

where:

S specific surface of the aggregate (m^2/kg),

w_0 water demand of aggregate, in case of natural sandy gravel aggregate it can be taken approximately as
$w_0 = 2.0$ m%, if the particle grading is continuous
$w_0 = 1.5$ m%, if the particle grading is gradual.

THANH [10] has also determined that the paste demand between the theoretical and practical paste saturation decreases with the increase of MSA that is with the decrease of the specific surface of sand.

For crushed andesites ZSIGOVICS [3] has found that for their water demand the formulas introduced for river sandy gravel by UJHELYI [8] can be used successfully.

BALÁZS [9] has verified the importance of paste-saturated concrete by several experiments.

During further experiments on prisms under compression we determined the stress-strain diagrams ($\sigma - \varepsilon_x$) in the direction of the load and ($\sigma - \varepsilon_y$) orthogonal to the load and calculated the stress-specific volume change diagram. Three basically different types of this can be differentiated (*Figure 1*):

1. type: following an initial linear compression the concrete's density increases and the crumbling process starts.
2. type: following an initial linear compression of the concrete, directly the crumbling process follows.
3. type: following an initial linear compression of the concrete it fails after the first slow, then a quick density increase process.

The applied measuring method and the internal stresses of unloaded specimen mostly can make trouble in the characters of fracture mechanism process. We eliminated this own stress of unloaded specimen with loading – de-loading process (*Figure 2*).

a) The initial values of ΔV are $1.25 - 4.40$.
b) The beginning of the volume decrease $(0.2 - 0.5)\,\sigma / R_{cpr}$.
c) The place of $\Delta V = 0(0.6 - 0.9)\sigma / R_{cpr}$.

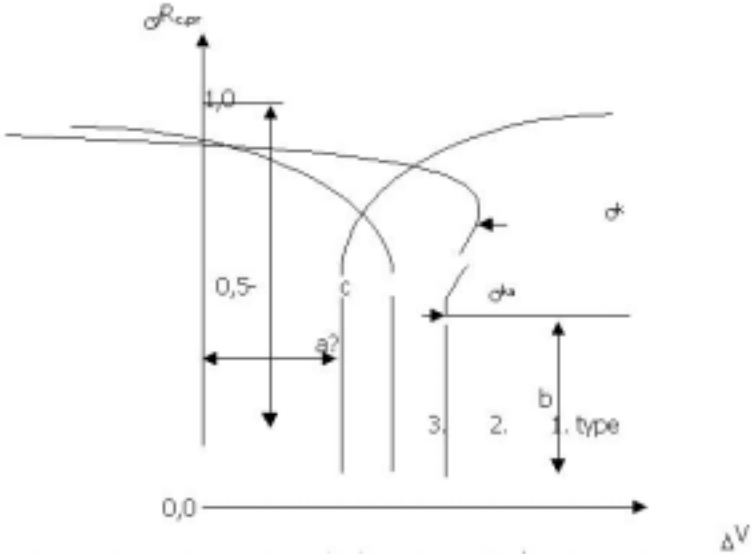

Fig. 1. The basic types of $\sigma / R_{c,pr} - \Delta V$ curves

On the *Figure 1* of the maximum value the 1. type graph is called σ_k by professor Rusch. Here begins the rapid failure of concrete and equals the long-term strength. The beginning of the volume change was named by Balázs σ_{ka}. According to his hypothesis the law of linear creep is valid until this point.

In the region of paste-saturated concretes prepared using aggregate following the A16 curve (max. 20– 25 l/m^3 over-saturation) σ_{ka} is:

in case of curing under water, ca. 0.8 σ / R_{cpr},
in case of curing in laboratory air, ca. 0.6 σ / R_{cpr},
in case of dried concrete, ca. 0.6 σ / R_{cpr}.

2. The Description of the Experiment

With the investigation, which we considered as a preliminary experiment, our aim was to estimate the limit of long-term loading until which the law of linear creep is valid (creep is proportional to the loading stress).

We prepared a high strength, paste-saturated concrete. At this time we also investigated how the stress vs. strain properties of young (2 – 3 days old) concrete will change under long-term loading. The knowledge of this is very important in case of some up to date technologies (e.g. bridge construction by free cantilever method by natural hardening).

The cement was 450R pc from Vác (new name: CEM I 42.5). Mineral composition:

AM: 1.55 m%
C_3S: 45.20 m%
βC_2S: 25.69 m%
C_3A: 8.55 m%
C_4AF: 10.80 m%

The standard physical properties of the cement:

Water demand: Water-cement ratio	0.287 m%
Beginning of set:	2 hours 20 minutes
End of setting:	4 hours 20 minutes
Sieve residue	
Retained on the 0.2 mm sieve:	0.05 m%
Retained on the 0.09 mm sieve:	1.25 m%
Specific surface:	345.2 m^2/kg
Density:	3.172 g/ml
Soundness by boiling:	acceptable

The standard strength of cement is given in *Table 1*.

Table 1. The standard strength of cement

Age in days	Average bending-tensile strength	Average compressive strength
	MPa	MPa
1	4.68	17.2
3	7.40	26.5
7	8.62	34.0
28	9.34	47.3

The aggregate was washed, dried, sandy gravel from River Danube, separated by fractions, the particle size distribution curve of which was between the A16-B16 boundary curves.

The gap volume of the aggregate skeleton was determined as follows:
For the determination of the gap volume we used a cylinder of ø150 $\times$ 300 mm. We mixed the dried aggregate fractions (0/1; 1/4; 4/8; 8/16) in the percentage ratios given by the experimental aggregate grading boundary curve. Then with a moisture content of 2, 4, 6, 8 volume% determined the bulk density of the mixture. We plotted a graph of bulk density against moisture content and determined the water demand belonging to the optimal vibrating time (compaction).

We considered the water keeping and water demand of the examined material optimal, when – following compaction – the moisture content was the same for the

samples taken from the top, the middle and the bottom of the cylinder. Knowing the bulk density we calculated the gap volume of the aggregate as follows:

$$V_h = 1 - \rho_h/\rho_a = 1 - t_a.$$

where:
V_h is the gap volume,
t_a is the solidity of the aggregate,
ρ_a is the density of the aggregate,
ρ_h is the bulk density.

By this method the gap volume of the experimental aggregate was about 240 l/m^3 (this was expressed by THANH [6] as theoretical paste saturation $V_{p,th}$), based on the results of our earlier experiments we estimated the practical paste saturation to be $V_{p,pr}$ 280 l/m^3 (paste excess 40 l/m^3). We have put this much paste into the concrete.

We used the plasticizer CHEM 611 LK distributed by CHEM BETON Ltd. in a 40% solution and 4 m% dose. We obtained silica powder from the Zagyvaróna Alloy factory.

The properties of the silica powder:

Physical properties:	
Specific surface according to Blaine:	2000 m^2/kg
Density:	2.29 kg/l
Chemical composition:	
Loss of glow:	1.08 m%
SiO_2:	94.7 m%
CaO:	0.62 m%
MgO:	0.22 m%
Fe_2O_3:	0.51 m%
Al_2O_3:	0.38 m%
SO_3:	1.28 m%

Constituents of concrete:

Cement (from the factory Vác) 450 Rpc:	460.0 kg/m^3
Water:	110.4 kg/m^3
Admixture (CHEM 611 LK):	28.4 (4m%)
Silica powder: (Elkem 940 UH):	46.0 (10m%)
Aggregate:	
0/1 fraction (25%):	464 kg/m^3
1/4 fraction (22%):	408 kg/m^3
4/8 fraction (20%):	371 kg/m^3
8/16 fraction (33%):	612 kg/m^3
ρ fresh concrete:	2490 kg/m^3
water-cement ratio:	$x = 0.4$
water-(cement+silica powder) ratio:	0.25

Table 2. Properties of fresh concrete

Series	Consistence			Pieces of specimens, pcs.		Density of fresh concrete
	K_t	k_r	k_{CF}	Cube	Prism	
	cm	mm	–	150 × 150 × 150	120 × 120 × 360	kg/m^3
1	37	125	0.910	6	5	2450
2	36	98	0.850	12	5	2456
3	38	147	0.935	13	5	2448
4	39	195	0.962	14	5	2444
5	36	195	0.914	14	5	2427
average	37	152	0.914	Total: 59	Total: 25	2445

We prepared the concrete mixture in DZ 50 type concrete mixer. At first the dry materials were mixed for 1 minute, then about 80% of the mixing water was added and mixed for a further 1 minute and finally added the admixture diluted with the remaining water and a further 1.5 minute mixing was applied.

At first we determined the properties of the fresh concrete (*Table 2*), then prepared the necessary sample specimens. In the table k_t is the value of spread, k_r is the slump value and k_{CF} is the compacting factor. With the water-cement ratio and the admixture we set the consistence to semi plastic.

Table 3. Designed and real values of load levels

Sign	Load level, σ/R_{crp}; (%)	
	Designed value	Real value
1	70	75.7
2	60	62.5
3	50	50.0
4	30	30.3

Using the cubes of $150 \times 150 \times 150$ mm we prepared, we determined the compressive strength of the concrete at the ages of 1, 2, 3, 7, 14, 28, 91 and 141 days. On the prisms of 120 × 120 × 360 mm at the age of 2 days when starting the long-term loading and later at the age of 28 and 147 days we determined the prism strength, the modulus of elasticity and the volume change function. The remaining 2–2 prisms were put into the long-term loading device (spring instrument) to determine the creep factor and to examine the shrinkage.

The designed and real long-term loadings compared to the prism strength we gave in *Table 3.*

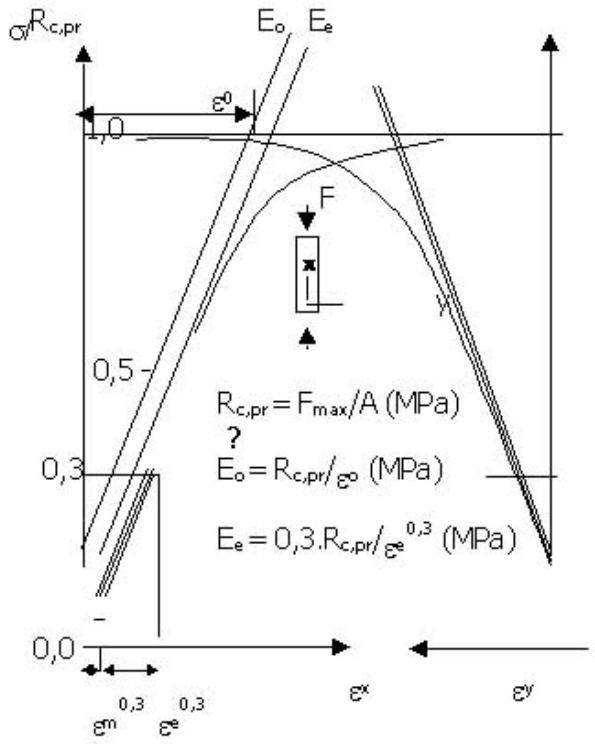

Fig. 2. Drawing and calculation of modulus of elasticity

3. Results of the Examination and Evaluation of the Results

3.1. Cube Strength

Following the removal of shuttering from the age of 1 day we kept the cubes under water until the time of examination. We tested cube compressive strength using Amsler 5000 kN instrument at the ages of 1, 2, 3, 7, 14, 28, 91 and 141 days.

According to the results of the examination following the age of 28 days the concrete practically had no post-hardening. This is partially due to the used rapid cement and partially due to the under-water curing. The average cube strength at the age of 2 days was 67.5 MPa while at the age of 28 days 96.1 MPa.

3.2. Failure Process (Prisms Which Were Not Loaded Previously)

The prisms of $120 \times 120 \times 360$ mm following the removal of the shuttering we kept for 2 days under water then at normal laboratory ambient conditions until the time

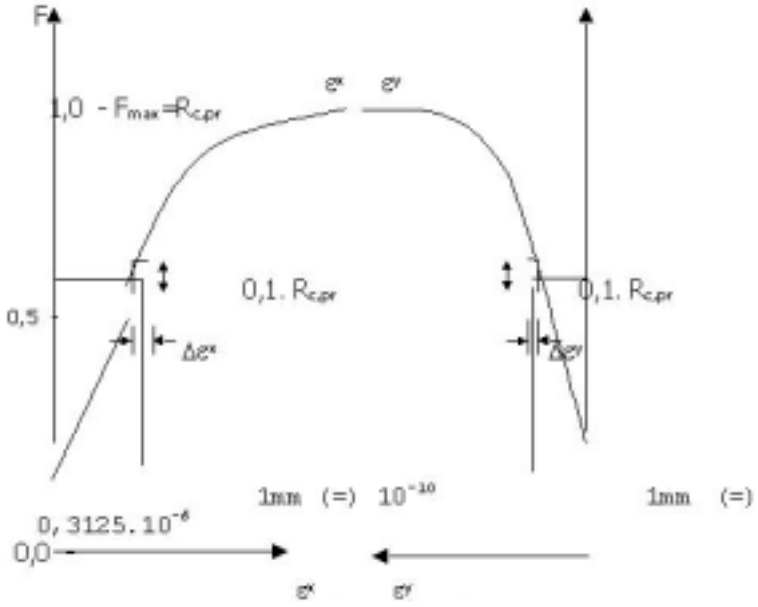

Fig. 3. Construction of $\Delta V - \sigma / R_{c,pr}$ function

of testing. We determined the prism strength and other failure factors at the age of 2, 28, and 147 days on prisms which were not loaded before. The examination results of the 2 days concrete are in *Table 4* while the 147 days results are given in *Table 5*.

On these samples we determined the mechanism of failure, the initial ($E_0 =$ zero starting point) modulus of elasticity and the modulus of elasticity after unloading (E_e). We carried out the loading in such a way that we unloaded from about 30, 50, 62 and 75% of the estimated prism strength. The unloading procedure was as follows: we loaded to the estimated level five times and kept it for about 10 minutes each. Following that we loaded the specimen till failure excluding the remaining deformation. The tangent of the last graph gives the modulus of elasticity (E_e). An example is shown on *Figure 4*.

Figure 2 also shows the calculation method of initial modulus of elasticity. The E_0 initial modulus of elasticity was calculated from the wrapping curve of the force-strain diagram, the E_e modulus of elasticity was determined from the curve of loading following the last unloading. From now we call E_0 and E_e as the modulus before unloading and after unloading.

During the examination on the two opposite plain surfaces of the $120 \times 120 \times 360$ mm prisms at the half of the height we placed D32 type 100 mm, and 80 mm base length induction elongation measuring devices. We draw the $\sigma_x - \varepsilon_x$ and $\sigma_x - \varepsilon_y$ functions using an $x - y - y'$ plotter for short-term static load. Together with

Table 4. The results of 120 × 120 × 360 mm unloaded prisms at the age of 2 days

The properties belonging to σ/R_{cpr} unloading levels. Age: 2 days								
Properties	30.3%			50%			62.5%			75.7%		
$R_{c.pr.}$ (MPa)	51.01	52.61	54.21	52.77	53.20	53.20	53.37	54.32	55.28	54.55	54.22	53.89
E_0 (MPa)	38940	39275	39609	38830	37548	36267	37453	37401	37350	35806	35305	34803
E_e (MPa)	38940	37452	35965	36267	37549	38830	37453	35968	34482	34350	34785	35221
ε_r (‰)	0.393	0.423	0.453	0.727	0.704	0.680	0.891	0.946	1.002	1.202	1.180	1.158
ε_x (‰)	1.770	1.785	1.800	2.110	1.905	1.700	2.000	2.000	2.000	1.83	1.88	1.83
ε_y (‰)	–	–	–	–	0.568	0.568	0.550	0.575	0.600	0.525	0.563	0.600
$\mu_{0.5}$	–	–	–	–	0.158	0.158	0.164	0.172	0.180	0.189	0.187	0.185
$\Delta V_{initial\ value}$ ($\cdot 10^{-5}$)	–	–	–	10.25	10.25	–	10.25	10.00	9.75	9.50	9.75	10.00
σ_{ka}	–	–	–	0.50	0.50	–	0.50	0.55	0.60	0.45	0.45	0.45
σ_k	–	–	–	0.80	0.80	–	0.90	0.90	0.90	0.80	0.80	0.80
Type of ΔV	1			1			1			1		

the cycles of loading-de-loading the time needed for failure was about 30 minutes.

We have divided the stress-strain diagrams to parts corresponding to $\Delta R = 0.1 \times R_{c,pr}$ (*Figure 3*), then calculated according to BÉRES [2] with correct ± sign in every point where the values of the relative volume changes using the formula:

$$\Delta V = \Delta V_e/\Delta R = (\Delta\varepsilon_x - 2\Delta\varepsilon_y)/\Delta R.$$

The values calculated we plotted in the $\Delta V - \sigma/R_{c,pr}$ coordinate system and connected the points with a continuous line, obtaining the $\Delta V - \sigma/R_{c,pr}$ functions.

Table 5. The results of 120 × 120 × 360 mm de-loaded prisms at the age of 147 days

The properties belonging to σ/R_{cpr} unloading levels. Age: 147 days				
Properties	30.3%	50.0%	62.5%	75.7%
$R_{c.pr.}$ (MPa)	89,58	83.33	86.81	90.28 91.32 92.36
E_0 (MPa)	45017	44803	44745	43403 45025 46647
E_e (MPa)	45017	44803	44745	43403 45025 46647
ε_e (‰)	0.663	0.930	1.213	1.575 1.537 1.499
ε_x (‰)	2.270	2.100	2.160	2.200 2.190 2.180
ε_y (‰)	0.455	0.495	0.385	0.455 0.463 0.470
$\mu_{0.5}$	0.138	0.167	0.145	0.150 0.160 0.170
$\Delta V_{initial\ value}(\cdot 10^{-5})$	14.50	12.00	13.50	13.60 13.80 14.00
σ_{ka}	0.40	0.50	0.60	0.70 0.75 0.80
σ_k	0.80	0.80	0.90	0.90 0.90 0.90
Type of ΔV	1	1	1	1

The characteristic points of the functions are shown in *Figure 1.*

The shape of $\Delta V - \sigma/R_{c,pr}$ function greatly depends on the structure of the concrete and the magnitude of strength. In our case the characteristic form of the function is according to the '1' type in *Figure 1.* We have summarized the characteristic values of the function in *Tables 4–5.*

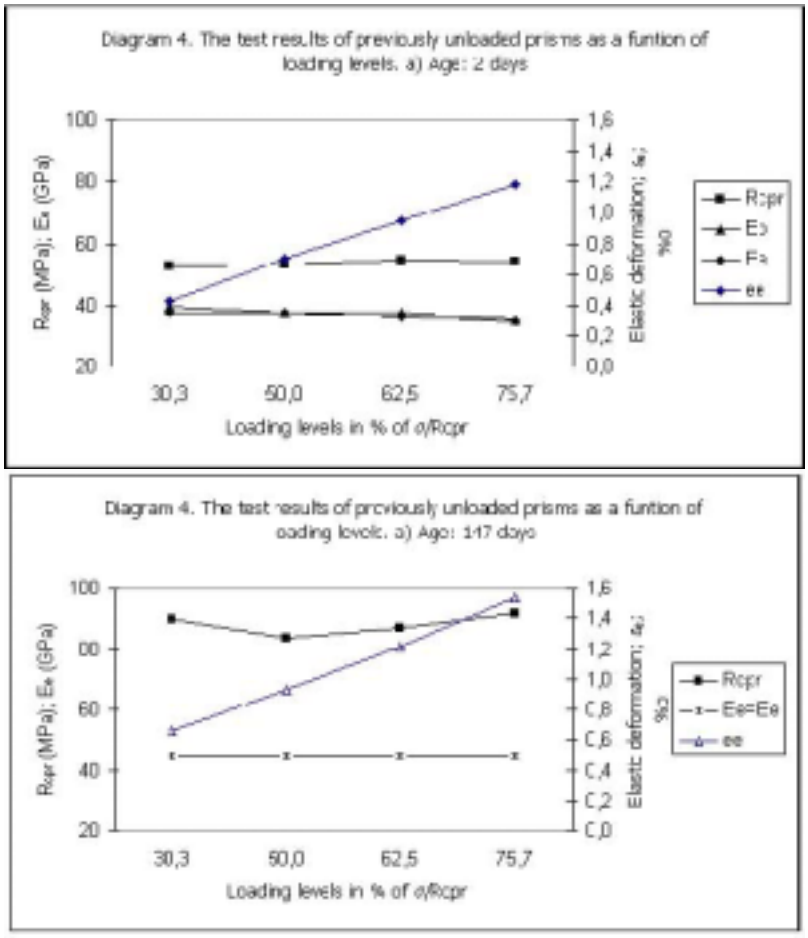

Fig. 4. The test results of previously unloaded prisms as a function of loading levels. a) Age: 2 days; b) Age: 147 days

Results of the Examination

a) The strength of the de-loaded prisms compared to the cube compressive strength is surprisingly big. In case of high strength concretes the assumed 3/4 ratio seems not valid and the ratio also depends on age.

Age of concrete:	2	28	147 days
Average prism strength:	53.6	82.4	87.7 MPa
Average cube strength:	67.5	96.1	97.2 MPa
Ratio:	79.4	85.4	90.3

b) We gave the values of strength, initial and unloaded modulus of elasticity and

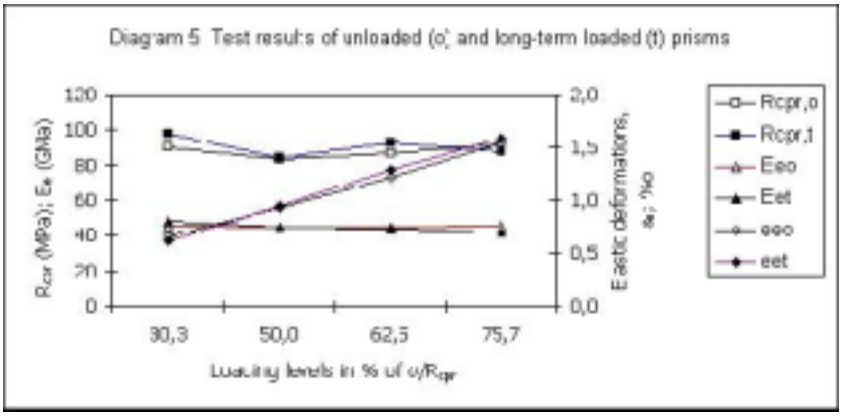

Fig. 5.

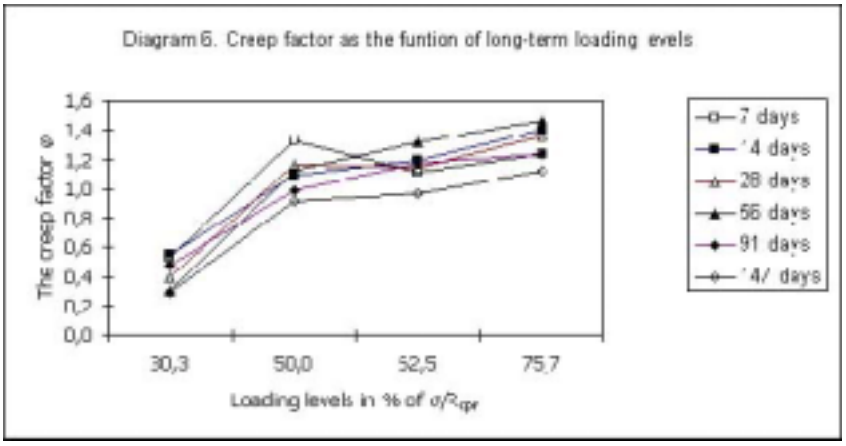

Fig. 6.

characteristic values of $\Delta V - \sigma / R_{c,pr}$ function with its nature of the prisms examined at the age of 2, 28, 147 days in *Tables 4–5* and on *Figs 4–7.*

- We de-loaded from higher level we obtained lower values for the modulus of elasticity, while the prism strength was nearly the same.
- The elastic deformations increased linearly by increasing the load levels.
- As the age increased so decreased the difference between the initial and de-loaded modulus of elasticity belonging to σ stress.
- The nature of $\Delta V - \sigma / R_{c,pr}$ function is of type '1' independently from the magnitude of the de-loading level. The initial value of the function

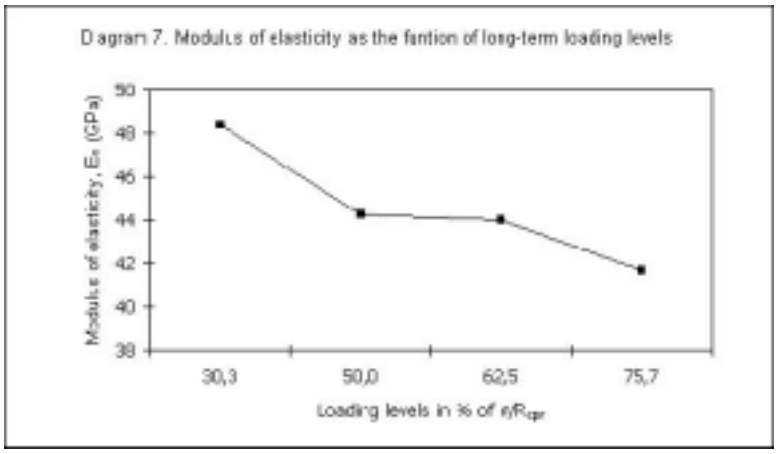

Fig. 7.

increased by the age of concrete. The magnitude of the constant part increased linearly with the age of concrete.

– The Poisson factor can be taken as a constant until 0.5 related stress value. Its value decreased with the increase of the age of concrete.

3.3. Shrinkage and Long-term Deformation

We determined the long-term deformation of concrete in spring equipment. The examination was prepared as follows: We determined the strength of 2–2 places of 2 days old 120 × 120 × 360 mm prism ($R_{c,pr}$), the modulus of elasticity (E_0 and E_e) and the failure-mechanical characteristics at the stress levels of $\sigma/R_{c,pr} = 0.3$; 0.5; 0.6 and 0.75. Following this we loaded in the springed instrument the two prisms – from identical series – with stress according to the above. The shrinkage of the concrete we measured by so-called one hundredths mm sensitive mechanical measuring clocks. The elongated measuring shafts of the clocks we fixed into one of the two measuring cams prepared for this purpose. The cams were glued in pairs to two smooth opposite sides of the prisms at a distance of about 210 mm adjusted to the half of the height in such a way that the measuring shaft is just touching the other cam. Following the loading we repeated the measurement at the age of 2, 3, 4, 5, 6 and 7 days later once or twice weekly.

Together with the long-term deformation we also measured the shrinkage of the same concrete. The long-term loading was terminated at the age of 147 days (21 weeks). Just after dismantling the spring device we determined the strength, the modulus of elasticity, the characteristics of the deformation and the characteristic values of the $\Delta V - \sigma/R_{c,pr}$ function of the prisms (*Table 6*).

Table 6. The results of 120 × 120 × 360 mm prisms following the long-term loading

The properties belonging to σ/R_{cpr} unloading levels. Age: 147 days				
Properties	30.3%	50%	62.5%	75.7%
$R_{c.pr.}$ (MPa)	96.18 97.98 99.79	86.81 84.03 81.25	93.40 92.88 92.36	87.50 87.50 –
E_0 (MPa)	48096 48388 48680	43400 44268 45136	44058 44020 43981	41667 41667 –
ε_e (‰)	0.605 0.613 0.621	1.000 0.950 0.900	1.250 1.282 1.313	1.590 1.590 –
ε_x (‰)	2.200 2.125 2.050	2.200 2.150 2.100	2.260 2.220 2.180	2.100 2.100 –
ε_y (‰)	0.495 0.553 0.610	0.700 0.695 0.690	0.480 0.543 0.605	0.750 0.750 –
$\mu_{0.5}$	0.150 0.157 0.163	0.187 0.177 0.167	0.150 0.159 0.167	0.167 0.167 –
$(\cdot 10^{-5})$ $\Delta V_{initial\ value}$	14.00 13.75 13.50	13.50 12.75 12.00	14.00 14.00 14.00	12.00 12.00 –
σ_{ka}	0.30 0.35 0.40	0.40 0.45 0.50	0.40 0.45 0.50	0.50 0.50
σ_k	0.80 0.80 0.80	0.80 0.80 0.80	0.90 0.85 0.80	0.80 0.80 –
Type of ΔV	1	1	1	1

We processed the results of the long-term testing to the results of the previously unloaded prisms. For comparison purposes we show together the properties of the previously unloaded and the long-term loaded prisms on *Figure 5.* At the age of 147 days of the concrete we checked the actual loading stresses in the spring devices (*Table 7*).

In *Table 8* we give an example for the results of the long-term loading experiments. We calculated the deformation arising from creep in such a way that from the value of total deformation at a given time we subtracted elastic deformation – calculated with the formula $\varepsilon_e = \sigma/E_e$ – and the shrinkage occurred from the time of loading till the measurement. We have characterized the creep with the creep factor (φ). By the creep factor we mean the quotient of at this given time the

Table 7. Actual loading stress value to the prism strength

Serial Number	Loading stress		Decrease of long-term loading, %
	At age of 2 days, MPa	At age of 147 days, MPa	
1	40.0	31.9	79.8
2	33.0	31.3	94.8
3	26.4	22.9	86.7
4	15.9	16.0	100.0

measured creep (ε_k) and at the time of loading the measured (calculated) elastic deformation (ε_e).

Conclusions derived from the result of the experiment:

- The strength of the long-term loaded concrete by less than 60% of the prism strength is 10% higher than the unloaded prisms. We explain this by the densening under the load.
- There is no difference in modulus of elasticity of the loaded prisms [initial (E_0) and after de-loading (E_e)]. This means that long-term loading eliminated the remaining deformation.

Date of Figure 5

Loading Levels %	$R_{cpr.o}$ MPa	$R_{cpr.t}$ MPa	E_{eo} GPa	E_{et} GPa	ε_{eo} ‰	ε_{et} ‰
30.30	89.58	97.89	45.02	48.39	0.66	0.61
50.00	83.33	84.03	44.80	44.27	0.93	0.95
62.50	86.81	92.88	44.75	44.02	1.21	1.28
75.70	91.32	87.50	45.03	41.67	1.54	1.59

Date of Figure 6

Loading Levels %	Creep factor φ					
	7 days	14 days	28 days	56 days	91 days	147 days
30.30	0.529	0.548	0.398	0.299	0.478	0.294
50.00	1.328	1.095	1.168	1.123	0.988	0.915
62.50	1.107	1.197	1.148	1.319	1.176	0.971
75.70	1.234	1.399	1.362	1.466	1.239	1.122

- Examining the load levels we can experience that the magnitude of the modulus of elasticity until 62.5% was equal to the ones of the previously unloaded prisms (*Table 8*) but at the 75.7% level it was about 8% less than the long-term loaded prisms.

Table 8. Results of long-term deformation measurements: Actual loading level 75.7%

Age	Sign of samples			Shrinkage			Creep		
	$V/1$	$V/5$	$V/1$	$V/5$	average	mm	%o	%o	factor
Days	Δ_l	Δ_l	ε_t	ε_t	ε_t	Δ_l	ε_{shr}	ε_{cr}	φ
2*	0.000	0.000	0.000	0.000	0.000	0.000	0.000	0.000	0.000
2	0.445	0.410	1.894	1.673	1.784	0.000	0.000	0.604	0.511
3	0.565	0.510	2.404	2.082	2.243	0.020	0.056	1.007	0.854
6	0.685	0.605	2.915	2.469	2.692	0.050	0.139	1.373	1.164
7	0.705	0.625	3.000	2.551	2.776	0.050	0.139	1.457	1.234
8	0.720	0.635	3.064	2.592	2.828	0.060	0.167	1.481	1.255
9	0.735	0.640	3.128	2.612	2.870	0.060	0.167	1.523	1.291
13	0.765	0.680	3.255	2.776	3.015	0.070	0.194	1.641	1.391
14	0.765	0.685	3.255	2.796	3.026	0.070	0.194	1.651	1.399
15	0.775	0.695	3.298	2.837	3.067	0.080	0.222	1.665	1.411
16	0.780	0.695	3.319	2.837	3.078	0.080	0.222	1.676	1.420
18	0.780	0.700	3.319	2.857	3.088	0.090	0.250	1.658	1.405
22	0.785	0.705	3.340	2.878	3.109	0.090	0.250	1.679	1.423
24	0.800	0.710	3.404	2.898	3.151	0.090	0.250	1.721	1.459
28	0.820	0.715	3.489	2.918	3.204	0.150	0.417	1.607	1.362
30	0.820	0.735	3.489	3.000	3.245	0.140	0.389	1.676	1.420
34	0.820	0.745	3.489	3.041	3.265	0.130	0.361	1.724	1.461
41	0.820	0.755	3.489	3.082	3.285	0.120	0.333	1.772	1.502
51	0.825	0.765	3.511	3.122	3.317	0.110	0.306	1.831	1.552
58	0.825	0.770	3.511	3.143	3.327	0.150	0.417	1.730	1.466
69	0.825	0.770	3.511	3.143	3.327	0.170	0.472	1.675	1.419
77	0.825	0.785	3.511	3.204	3.357	0.200	0.556	1.622	1.374
85	0.825	0.785	3.511	3.204	3.357	0.240	0.667	1.511	1.280
98	0.835	0.805	3.553	3.286	3.419	0.280	0.778	1.462	1.239
107	0.840	0.807	3.574	3.294	3.434	0.300	0.833	1.421	1.204
119	0.845	0.814	3.596	3.449	3.522	0.320	0.889	1.453	1.232
127	0.846	0.817	3.600	3.335	3.467	0.340	0.944	1.343	1.138
133	0.850	0.817	3.617	3.335	3.476	0.340	0.944	1.351	1.145
147	0.850	0.817	3.617	3.335	3.476	0.350	0.972	1.324	1.122

Where: 2* before long-term loading,
Elastic deformation: $\varepsilon_e = 1.180$%o
Remaining deformation: $\varepsilon_m = 0.604$%o
$\varepsilon_{cr} = \varepsilon_t - \varepsilon_e - \varepsilon_{shr}, \quad \varphi = \varepsilon_{cr}/\varepsilon_e$
base length: $l_0(II/1) = 235$ mm,
base length: $l_0(II/4) = 245$ mm

– The measured elastic deformation has increased linearly to the different loading and de-loading levels (*Table 9*).

Table 9. Elastic deformation is proportional to the loading level

Load levels	30%	50%	62.5%	75.7%
their ratio:	1.00	1.67	2.08	2.52
Elastic deformation	0.613%	0.950%	1.282%	1.590%
their ratio:	1.00	1.55	2.09	2.59

- The value of the total longitudinal deformation (ε_x) belonging to failure in both the unloaded and the long-term loaded case of the prisms was 2–2.1%. However, the orthogonal deformation was 0.55–0.75% in case of the long-term loaded prisms. This is 20–30% bigger than the unloaded prisms. The effect of this is experienced at lower level (instead of 0.60–0.80 between 0.45–0.50) and σ_{ka} will occur.
- The long-term loading until the 50% load level has increased the value of Poisson factor ($\mu_{0.5}$) by 5–10% comparing to the unloaded prisms.
- The stress level, causing failure (ε_k) both in the long-term loaded and unloaded prisms case was the same (about 0.80).
- In case of all 4 series the shrinkage value of the same mixture but different mixing time has reached the level of 1‰.
- In *Figure 6* we illustrate the creep factors against the load levels at the age of 7, 14, 28, 56, 91 and 147 days. We can experience that the creep factor will deviate over the 50% load from the linear function. It is also an experience from our experiments that in following experiments we must place one more step between the 30–50% load levels.
- *Figure 7* shows a decreasing tendency of the modulus of elasticity by the increase of load levels, which can with a good approximation be expressed as a linear function.

4. Summary

We have prepared high strength concrete and we examined the strengthening process using cubes. Then the 120 × 120 × 360 mm prisms at the age of 2 days were long-term loaded to about 30, 50, 62 and 75% of their prism strength and the creep factor was determined. Further we have determined the prism strength, the initial (E_0) and the (E_e) modulus of elasticity the latter of which belongs to load levels, the elastic deformation (e_e), Poisson factor ($\mu_{0.5}$), the diagram of volume change and its significant values of both the previously unloaded and following unloaded in case of the long-term loaded prisms.

The strength of the prisms long-term loaded by less than 60% stress – due to densening – has increased by 5–10%.

The failure value $\sigma_k = 0.8$ in case of both the long-term loaded and the unloaded prisms. By the increase of the age, the value of e σ_{ka} increased. The

long-term loading decreased the value of σ_{ka} to 0.35–0.5. The creep factor proportionally increases until about $0.5\sigma / R_{c,pr}$ value with the loading stress, so most probably until σ_{ka} is valid the law of linear creep, but this hypothesis must be proved by further experiments.

Acknowledgements

This research was supported by the Hungarian National Scientific Research Foundation (OTKA), Grant No. T016686. Authors are grateful for funding and continuous support of OTKA.

References

[1] FERET, R.: Sur la compacite des mortiers hydrauliques. *Annales des Ponts et Chaussées*, Paris, No. 1. (1892) pp. 1–184.
[2] ABRAMS, D. A. (1918): Design of Concrete Mixture Bulletine, No. 1. Structural Materials Research Laboratory. Lewis Institute, Chicago.
[3] PALOTÁS, L.: Verfahren zur Verbesserung Betonzuschlagstoffe. *Zement*, (1936) Heft 18.
[4] UJHELYI, J.: A beton struktúrájának és nyomószilárdságának tervezése. Akadémiai doktori értekezés.
[5] BALÁZS, GY.: A betontulajdonságok a betonstruktúra függvényében. Építőanyagok Tanszék Tudományos Közlemények **36** (1982) 1. pp. 81–125.
[6] NGUYEN HUU THANH (1986): Ferrocement betonjának tervezése. Kandidátusi értekezés.
[7] ZSIGOVICS, I. (1987): A péptelítettséghez szükséges pépigény meghatározása zúzott adalékanyag esetére. BME Építőanyagok Tanszéke, Kutatási jelentés.
[8] BALÁZS, GY.: Der Zementstättigungswert als eine wichtige Kenngröße der Betonstruktur. *Baustoffe*, (1985) pp. 5–6.
[9] BALÁZS, GY. – ZSIGOVICS, I. (1985): A beton tulajdonságai a struktúra függvényében II. Az ÉVM megbízásából készített kutatási jelentés.
[10] NGUYEN HUU THANH: Optimal Concrete Composition Based on Paste Content for Ferrocement. *Journal of Ferrocement.*. **21**, (1991)No. 4, October.
[11] NGUYEN HUU THANH: Fracture Mechanism of Ferrocement Depending on Paste content. *Journal of Ferrocement.* **22**, (1992) No. 2, April.